iScience

CellPress
OPEN ACCESS

Article

CT135 mediates the resistance of *Chlamydia trachomatis* to primate interferon gamma stimulated immune defenses

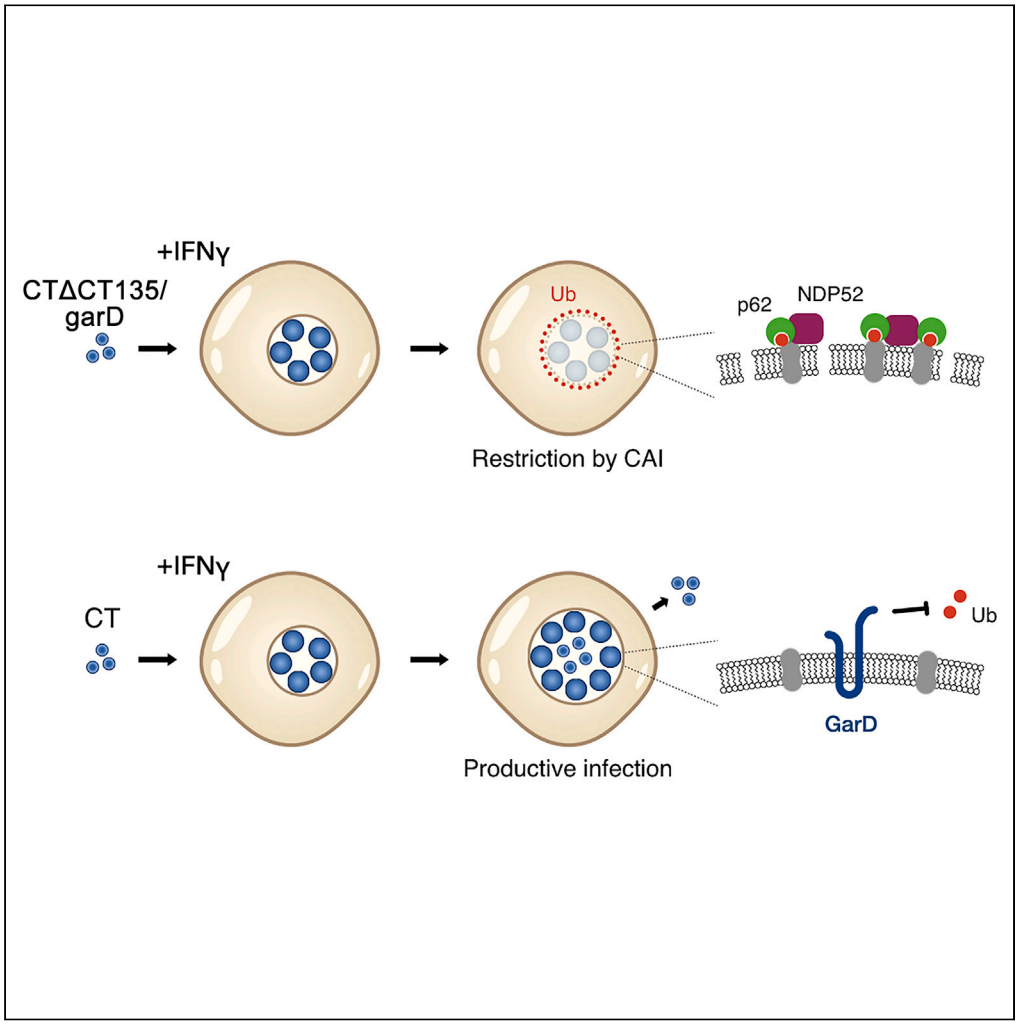

Mark C. Fernandez, Yvonne Cosgrove Sweeney, Robert J. Suchland, ..., Daniel D. Rockey, Dorothy L. Patton, Kevin Hybiske

khybiske@uw.edu

Highlights

CT135/GarD mediates *C. trachomatis* interference with cell-autonomous immune defenses

CT135/GarD prevents the targeting of ubiquitin to *C. trachomatis* inclusions

The action of CT135/GarD is conserved between humans and nonhuman primates

CT135/GarD mutants are attenuated for growth in nonhuman primates

Fernandez et al., iScience *27*, 110143
June 21, 2024
https://doi.org/10.1016/j.isci.2024.110143

iScience

CellPress
OPEN ACCESS

Article

CT135 mediates the resistance of *Chlamydia trachomatis* to primate interferon gamma stimulated immune defenses

Mark C. Fernandez,[1,2] Yvonne Cosgrove Sweeney,[3] Robert J. Suchland,[4] Steven J. Carrell,[5] Olusegun O. Soge,[1,4] Isabelle Q. Phan,[6,7] Daniel D. Rockey,[5] Dorothy L. Patton,[3] and Kevin Hybiske[2,4,8,*]

SUMMARY

Evading host innate immune defenses is a critical feature of *Chlamydia trachomatis* infections, and the mechanisms used by *C. trachomatis* to subvert these pathways are incompletely understood. We screened a library of chimeric *C. trachomatis* mutants for genetic factors important for interference with cell-autonomous immune defenses. Mutant strains with predicted truncations of the inclusion membrane protein CT135 were susceptible to interferon gamma-activated immunity in human cells. CT135 functions to prevent host-driven recruitment of ubiquitin and p62/SQSTM to the inclusion membrane. In a nonhuman primate model of *C. trachomatis* infection, a CT135-deficient strain was rapidly cleared, highlighting the importance of this virulence factor for *C. trachomatis* pathogenesis. Analysis of CT135 phenotypes in primary macaque cells revealed that cell-autonomous immune defenses against *C. trachomatis* are conserved between humans and nonhuman primates and connects mechanistic findings with *in vivo* infection outcomes.

INTRODUCTION

Successful infection by *C. trachomatis* (CT) requires invasion of host epithelial cells and avoidance of the varied arms of innate immune defenses. As obligate intracellular pathogens, a key component of *Chlamydia* pathogenesis involves disrupting the multipronged antibacterial mechanisms activated in response to interferon gamma (IFNγ).[1] An emerging aspect of the innate, or cell-autonomous, host response against *Chlamydia* infection is the recognition of the *Chlamydia*-containing vacuole (termed the inclusion), decorating proteins on the inclusion membrane with ubiquitin, and targeting the bacteria for degradation by autophagy-related pathways.[2,3] Like other intracellular pathogens, *Chlamydia* have evolved potent host-adapted countermeasures against these host defenses.[1] These pathogenesis strategies are likely major contributors to CT pathogenesis and virulence due to the noted role of IFNγ in the host response to CT infection.[4] The specific chlamydial factors responsible for disrupting these mechanisms remain undiscovered. We leveraged a new library of CT × *C. muridarum* (CM) chimeric hybrid strains to identify and characterize a chlamydial inclusion membrane protein whose secretion onto the CT inclusion membrane is responsible for promoting bacterial growth and infectious elementary body (EB) production in the presence of IFNγ. We show that CT mutants lacking intact CT135 were attacked and restricted by IFNγ-activated defenses *in vitro* and were rapidly cleared in the reproductive tracts of female pig-tailed macaques.

RESULTS

Identification of a genetic locus required for CT resistance against cell autonomous immunity

The species-specific differences for CT and CM susceptibility to IFNγ-activated defense pathways afforded an opportunity to leverage our large library of chimeric CT mutants—containing homologous exchange of >80% of the CT and CM genomes—to map the allele(s) responsible for these phenotypes.[5] We screened 13 chimeras from the library in a microscopy-based assay to identify mutants that were unable to prevent inclusion ubiquitination in IFNγ-stimulated human epithelial cells (Figure 1A). 40.9% of CM inclusions were targeted by ubiquitin in IFNγ-primed A549 cells, whereas CT inclusions were devoid of ubiquitin (Figures 1B and 1C). Two initial mutant strains (RC435 and RC141) exhibited phenotypes that mirrored the sensitivity of CM, 33.2% and 37%, respectively (Figures 1B and 1C). These chimeras encode 75 and 71 recombined genes, respectively, and share an overlapping locus of 37 CM genes. To explore this chromosomal region further, we tested four

[1]Department of Global Health, University of Washington, Seattle, WA 98109, USA
[2]Center for Emerging and Re-emerging Infectious Diseases, University of Washington, Seattle, WA 98109, USA
[3]Department of Obstetrics and Gynecology, University of Washington, Seattle, WA 98109, USA
[4]Department of Medicine, University of Washington, Seattle, WA 98109, USA
[5]Department of Biomedical Sciences, Oregon State University, Corvallis, OR 97331, USA
[6]Seattle Structural Genomics Center for Infectious Disease, Seattle, WA 98109, USA
[7]Center for Global Infectious Disease Research, Seattle Children's Hospital, Seattle, WA 98109, USA
[8]Lead contact
*Correspondence: khybiske@uw.edu
https://doi.org/10.1016/j.isci.2024.110143

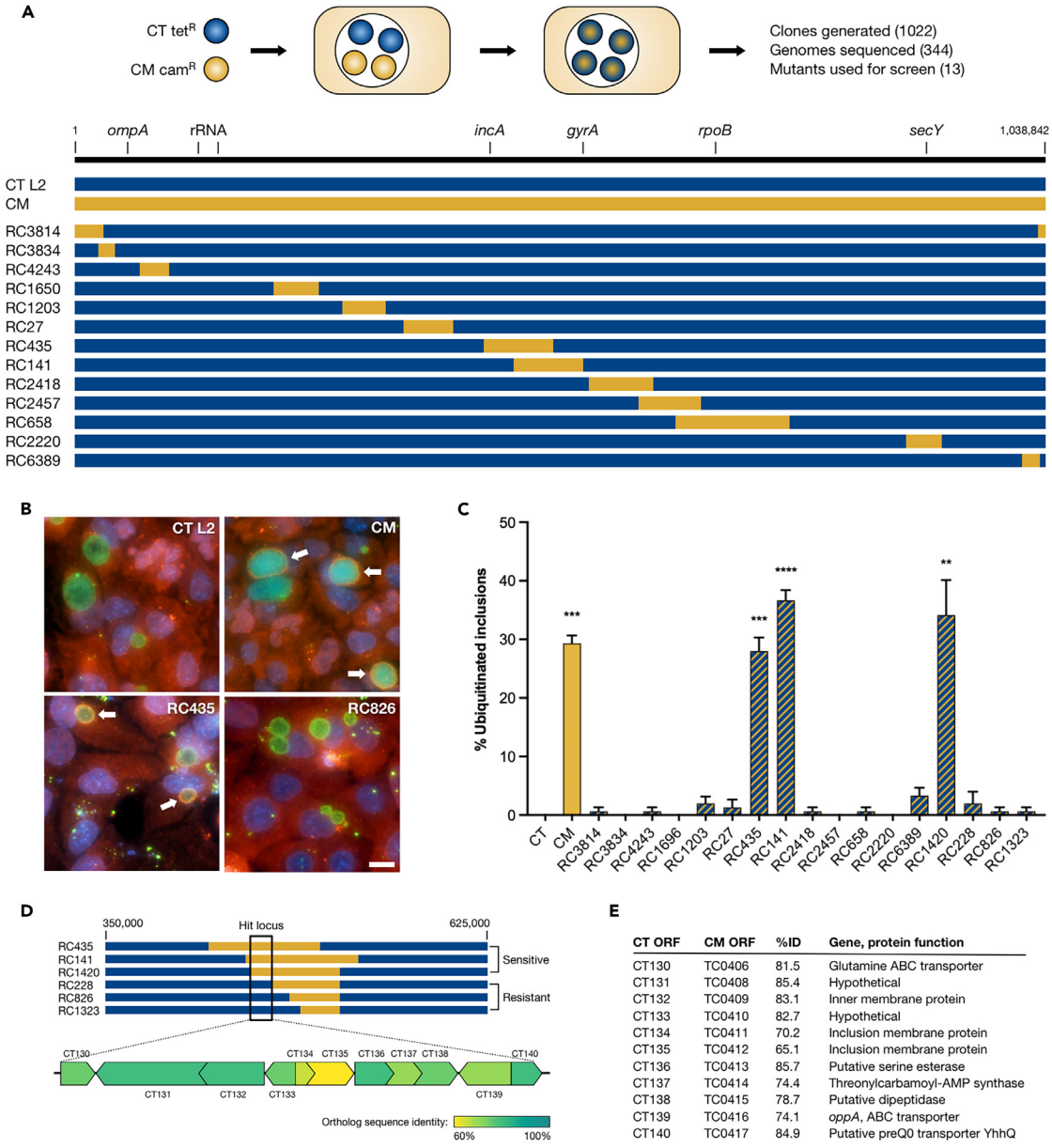

Figure 1. Genetic screen of *C. trachomatis* chimera library mutants susceptible to IFNγ-activated, cell-autonomous immune defenses

(A) Approach used to generate the CT × CM chimera mutant library, and linear genome maps depicting the 13-strain library used for screening (CT DNA, blue; CM DNA, orange).

(B) Visual screen for cell-autonomous immunity-susceptible strains in IFNγ-activated human A549 cells by measuring recruitment of ubiquitin (red) to *Chlamydia*-containing inclusions (green) at 20 hpi. Host nuclei labeled with DAPI (blue). Arrows indicate ubiquitinated inclusions. Scale bar, 20 μm.

(C) Screen of wild type CT-L2, CM, and 17 CT chimera mutants for susceptibility to IFNγ-activated targeting of ubiquitin to inclusion membranes (mean ± SEM, $n = 3$, unpaired Student's t test).

(D) Hit locus identified from comparative genomic analysis of sensitive and resistant chimera strains, with enlarged map of the 11 candidate genes contained in this locus. Gene colors denote amino acid sequence identity between CT and CM reference genomes.

(E) Tabulated summary of candidate genes.

sibling chimeras with unique recombination ends and identified an additional mutant (RC1420) defective in resisting cell autonomous defenses (Figure 1D). Comparative genomic analysis of phenotypic strains led to the identification of a 11 gene locus responsible for conferring resistance to IFNγ-activated immune defenses (Figure 1D). The gene encoded by *ct135* represented the highest amino acid sequence divergence between CT and CM within this locus (65.1%, Figures 1D and 1E), and we hypothesized its potential role in the described phenotype due to its preliminary characterization as a type III secreted inclusion membrane protein (Figure 1E).[6]

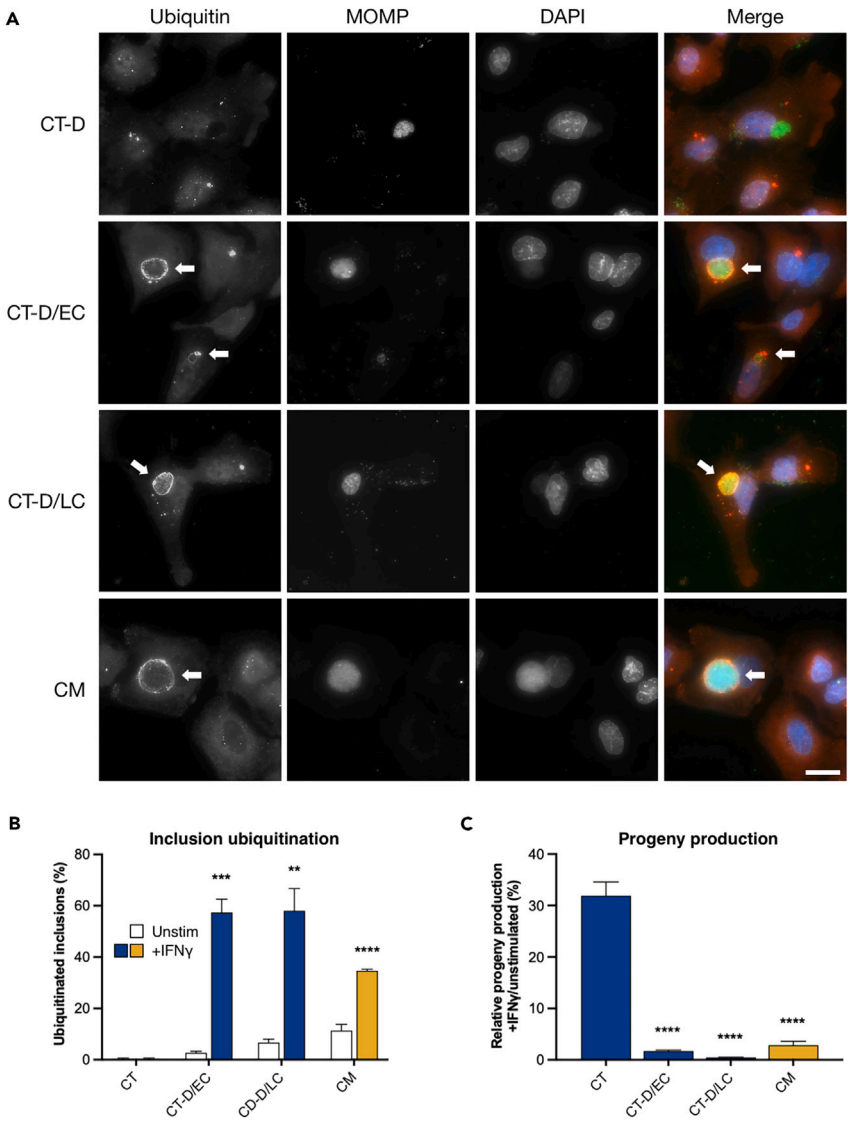

Figure 2. CT strains with frameshift mutations in CT135 are susceptible to cell-autonomous immune defenses in human cells

(A) Recruitment of ubiquitin (anti-ubiquitin, red) to inclusions containing CT-D strains with frameshift mutations in CT135 (CT-D/EC and CT-D/LC; anti-MOMP, green), and CM inclusions, in IFNγ-primed A549 cells at 20 hpi. Arrows indicate ubiquitinated inclusions. Scale bar, 20 μm.

(B) Quantitative assessment of inclusion ubiquitination to CT, CT135 frameshift mutant, and CM inclusions in unstimulated and IFNγ-activated cells (mean ± SEM, $n = 3$, unpaired Student's t test).

(C) Abrogation of CT135 mutant and CM growth in IFNγ-activated A549 cells was determined by assaying the amount of infectious *Chlamydia* EBs (IFUs) at 27 hpi. Cultures were supplemented with tryptophan to mitigate the effects of IFNγ-induced IDO. Values represent the ratio (%) of IFUs produced under +IFNγ to unstimulated conditions (mean ± SEM, $n = 3$, one-way ANOVA).

CT strains with frameshift mutations in *ct135* are susceptible to cell autonomous immunity

To investigate the contribution of CT135 to CT resistance against ubiquitin-mediated, cell-autonomous immune pathways, we obtained and tested two CT strains with documented frameshift mutations in *ct135*, CT-D/EC and CT-D/LC.[7] In addition to mutations in *ct135*, these strains harbor 17 shared polymorphisms in their respective genomes.[7] We found that in IFNγ-stimulated A549 cells, 51.9% and 58.5% of D/EC and D/LC inclusions were targeted with ubiquitin compared to 0% of inclusions containing wild type CT-D (Figures 2A and 2B). These outcomes were dependent on activation with IFNγ (Figure 2B). To determine the restrictive outcome of this phenotype, we measured the production of infectious EB progeny of mutant strains under IFNγ-activated and unstimulated conditions. These experiments were performed in tryptophan supplemented conditions to mitigate the inhibitory effects of indoleamine-2,3-dioxygenase.[3,8] We observed a significant inhibition of EB progeny production in IFNγ-primed cells infected with either CT135 mutant strains or CM, 1.7%, 0.5%, and 2.8%, respectively (Figure 2C). These phenotypes were significantly less than the 31.9% observed for wild type CT-D (Figure 2C).

Together, these data support a major role for the CT135 protein in facilitating the resistance of CT to IFNγ-activated, cell-autonomous defense mechanisms.

CT135 mutants lose virulence in a nonhuman primate model of CT infection

Parallel to the genetic screen discussed previously, we evaluated the infectivity and pathogenesis of two low passage CT isolates in the characterized female pig-tailed macaque model.[9] We inoculated animals with CT-D/6319 or CT-J/p225 strains and longitudinally assessed infection by nucleic acid amplification testing (NAAT) of cervical swabs, seroconversion by serum IgG titers, and recovery of CT organisms from weekly swabs for culturing and whole genome sequencing (Figure 3A). Animals infected with CT-D/6319 (n = 6) were positive for infection at week 1 by NAAT, and uncharacteristic clearance of CT-D was found in 2 of 6 animals by 5 weeks post infection (wpi) despite high seroconversion (Figure 3B). Only 4 animals were positive at 1 wpi by culture (Figure 3B). Animals infected with CT-J/p225 were reliably infected; all animals tested positive by culture or NAAT throughout the 5-week study (Figure 3C). To determine why CT-D failed to establish a reliable infection, we performed whole genome sequencing on the day 0 inocula and 5 wpi samples from both infection cohorts, and we evaluated whether inoculum preparations and samples remained homogeneous throughout the study. We identified 3 polymorphisms in the sequenced CT-D samples, all of which fell within the *ct135* gene. Three variant alleles were identified: a synonymous mutation at nucleotide 1034 (1.0% of day 0 reads, 17.3% of 5 wpi reads), a R284Q amino acid substitution (16.7% of day 0 reads, 78.9% of 5 wpi reads), and an adenine deletion at nucleotide 541 that resulted in a frameshift and early stop codon (32.0% of day 0 reads, 0% of 5 wpi reads) (Figures 3B, 3D, and S1). The frameshift mutation (ΔCT135) was not present in the 5 wpi sample, indicating that this population failed to establish a productive infection in NHPs. Furthermore, we were unable to detect the ΔCT135 allele in the 1–4 wpi samples by PCR sequencing (data not shown). The presence of *ct135* mutations in low passage clinical strains is not surprising given the documented selective pressure for spontaneous mutation at this open reading frame during adaptation of clinical isolates to *in vitro* culture.[10] Sequencing of CT-J samples identified a single chromosomal polymorphism that also fell within *ct135*. This L361F mutation was represented equivalently across day 0 and 5 wpi study samples (50.0% for both), indicating no *in vivo* selective pressure against this variant allele (Figure 3C). From this study, we hypothesized that reduced CT-D/6319 infectivity in macaques was due to the presence of a ΔCT135 mutant in the inoculum preparation that lowered the effective infectious titer of wild type CT-D, and a failure of the ΔCT135 mutant to overcome IFNγ-stimulated immune responses *in vivo*.

To test the mechanistic basis of this hypothesis, we analyzed the phenotypes of archived CT-D/6319 samples from the NHP study in human cells under IFNγ-activated or unstimulated conditions. These experiments revealed that 14% of inclusions from the CT-D/6319 inoculum population were targeted with ubiquitin (Figures 3D and 3E). The 5 wpi sample was targeted in just 3.3% of inclusions (Figures 3D and 3E). Ubiquitin targeting required cell activation with IFNγ; only 1% and 0% of inclusions from day 0 and 5 wpi samples, respectively, were positive for ubiquitin recruitment in unstimulated cells (Figures 3D and 3E).

CTΔCT135 mutants are impaired in resisting cell autonomous immune defenses

We isolated the ΔA541 frameshift mutant (CTΔCT135) and a clone containing the R284Q mutation from the CT-D/6319 inoculum via limiting dilution. We analyzed the cell-autonomous immunity resistance phenotypes of these clones under IFNγ-activated conditions, and we found that 60% of CTΔCT135 inclusions were targeted with ubiquitin in IFNγ-primed human cells compared to 1.3% in unstimulated cells (Figures 4A and 4B). The R284Q mutant exhibited a lower rate of inclusion ubiquitination, with only 8% of inclusions targeted in IFNγ-stimulated cells compared to 0% in unstimulated cells (Figures 4A and 4B). We restored the *ct135* ORF into the CTΔCT135 in *cis* using a backcrossing approach that recombined an intact *ct135* allele from CT-L2 (ortholog *ctl0390*) in exchange for the frameshift allele in the CTΔCT135 strain (Figure S2). This rescued strain (CTΔCT135::CT135) encodes a hybrid *ct135* ORF with *ctl0390* nucleotides in the 5′ region and *ct135* the 3′ region (nt1-558 and nt657-nt1080, respectively, Figure S3), which complemented the frameshift mutation within CTΔCT135 (Figure S3). This complementation rescued the ability of CTΔCT135::CT135 to resist IFNγ-activated defenses, as only 2% of its inclusions were found to be positive for ubiquitin targeting (Figures 4A and 4B). The CTΔCT135 (oflR, olfloxacin resistant) parent used to generate the complemented strain was susceptible to IFNγ-dependent targeting, with 50% of its inclusions being ubiquitinated in stimulated cells (Figures 4A and 4B). To better understand the impact of the CTΔCT135 frameshift mutation on the predicted CT135 protein, we performed AlphaFold2-advanced modeling[11,12] of the full length CT135 sequence, and determined that the bottom half of the alpha-helical bundle is hydrophobic and likely comprises the transmembrane region of the protein, while the surface of the C-terminal domain is highly hydrophilic and likely exposed to the surface above the membrane bilayer (Figure S4). The location of the ΔCT135 frameshift mutation in these models supports a truncation between the predicted transmembrane and C-terminal regions of the protein.

We next tested the ability of CTΔCT135 to colonize and infect the female reproductive tract (FRT) of macaques by infecting animals with inocula that were completely composed of the CTΔCT135 clone. One animal received a single inoculum and two animals received 5 sequential inoculations with the mutant. Quantification of recovered bacteria from weekly cervicovaginal swabs showed poor infectivity of the CTΔCT135 mutant in macaque FRTs (Figure 3F). Peak infectious burdens of 210 inclusion forming units (IFU) were obtained at 1 wpi for the animal that received a single infection, and only 14 IFU for animals that were serially infected. The CTΔCT135 was effectively cleared by 2 wpi. These results were in stark contrast to animals infected with the isogenic CT-D/6319 inoculum, where peak infectious burdens of 816 IFU were measured at 1 wpi and infections were sustained out to 5 wpi (Figure 3F). IFU analyses were performed in IFNγ-free tissue culture conditions so that mutant *in vitro* growth would not be impeded. NAAT testing of weekly cervicovaginal swabs acquired in parallel showed positive tests for all animals at 1 wpi (Figure 3F). Positive NAATs decreased to 2 animals at 2 wpi and 1 animal at 5 wpi. The animal which received a single inoculum of CTΔCT135 was NAAT positive only at week 1.

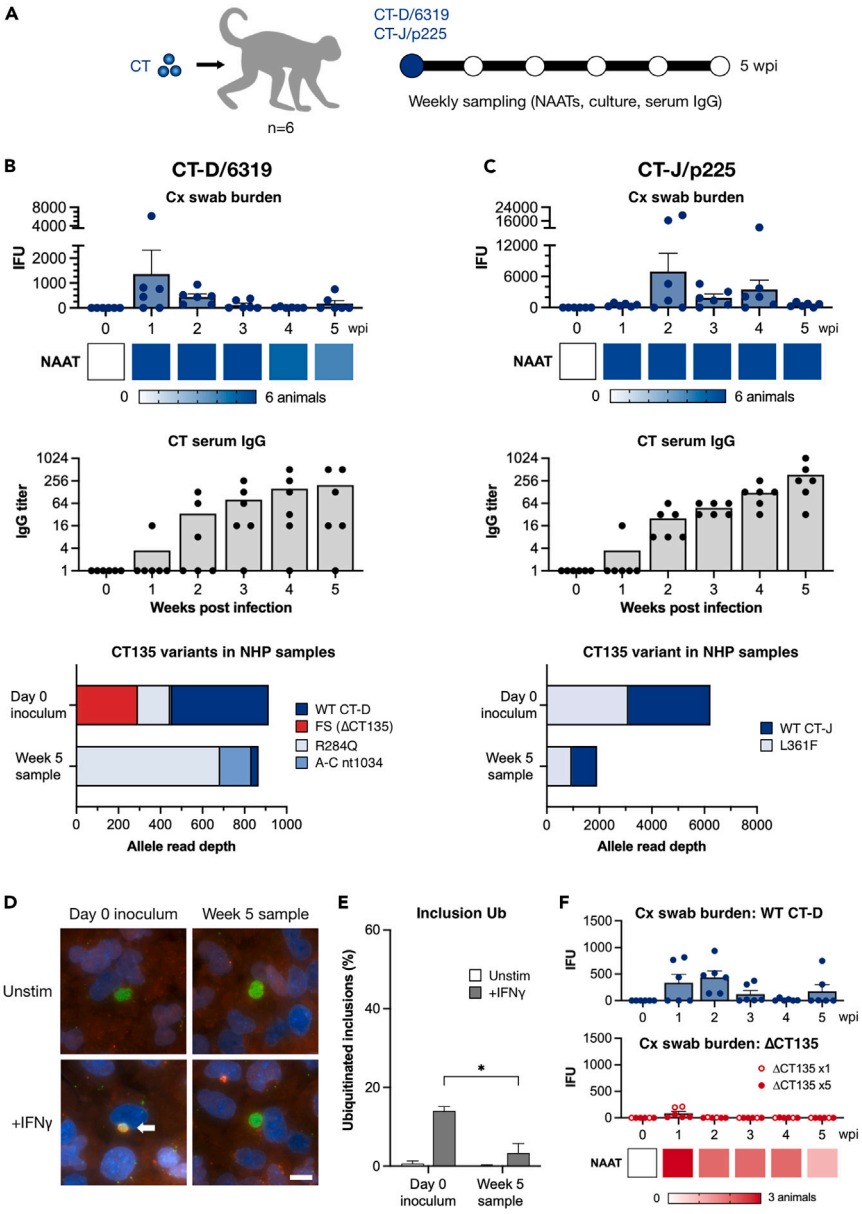

Figure 3. CT135 mutants lose virulence in a nonhuman primate model of *Chlamydia* infection

(A) Overview of CT-D and CT-J challenge of macaques ($n = 6$) and weekly sampling schedule for NHP infections.

(B and C) Data from animals challenged with CT-D/6319 or CT-J/p225. Top: infection positivity at weeks 0–5 as measured by culture (mean ± SEM) and NAAT analysis of cervical swabs. Middle: seroconversion by longitudinal anti-CT serum IgG titers (mean ± SEM). Bottom: SNPs in the CT135 gene identified by whole genome sequencing of day 0 inoculum and week 5 cervical samples.

(D) *In vitro* cell-autonomous immunity phenotypes (A549 cells ± IFNγ, 20 hpi) of the day 0 inoculum and week 5 cervical samples from CT-D/6319 NHP experiments (anti-ubiquitin, red; anti-MOMP, green; DAPI, blue). Arrows indicate ubiquitinated inclusions. Scale bar, 20 μm.

(E) Evaluation of susceptibility of CT-D/6319 *in vivo* samples to cell-autonomous immune defenses in A549 cells (mean ± SEM, $n = 3$, unpaired Student's t test).

(F) Longitudinal bacterial burdens of weekly cervical swabs from animals infected with CT-D/6319 (top, mean ± SEM) or a pure inoculum of ΔCT135 (bottom, mean ± SEM); hollow red circles, single infection with ΔCT135 ($n = 1$); filled red circles, animals serially infected 5x with ΔCT135 ($n = 2$). NAAT results for ΔCT135 infected animals also shown.

IFNγ-dependent recruitment of p62/SQSTM to CTΔCT135 inclusions

The canonical autophagy protein p62/SQSTM is recruited to *Chlamydia* inclusions and other pathogen containing vacuoles (PCVs) following their labeling with ubiquitin in IFNγ-stimulated human and mouse cells.[2,13,14] In the mouse model of *Toxoplasma gondii* infection, p62 recruitment to PCVs enhances antigen presentation by major histocompatibility complex I (MHCI) which in turn promotes $CD8^+$ T cell activation

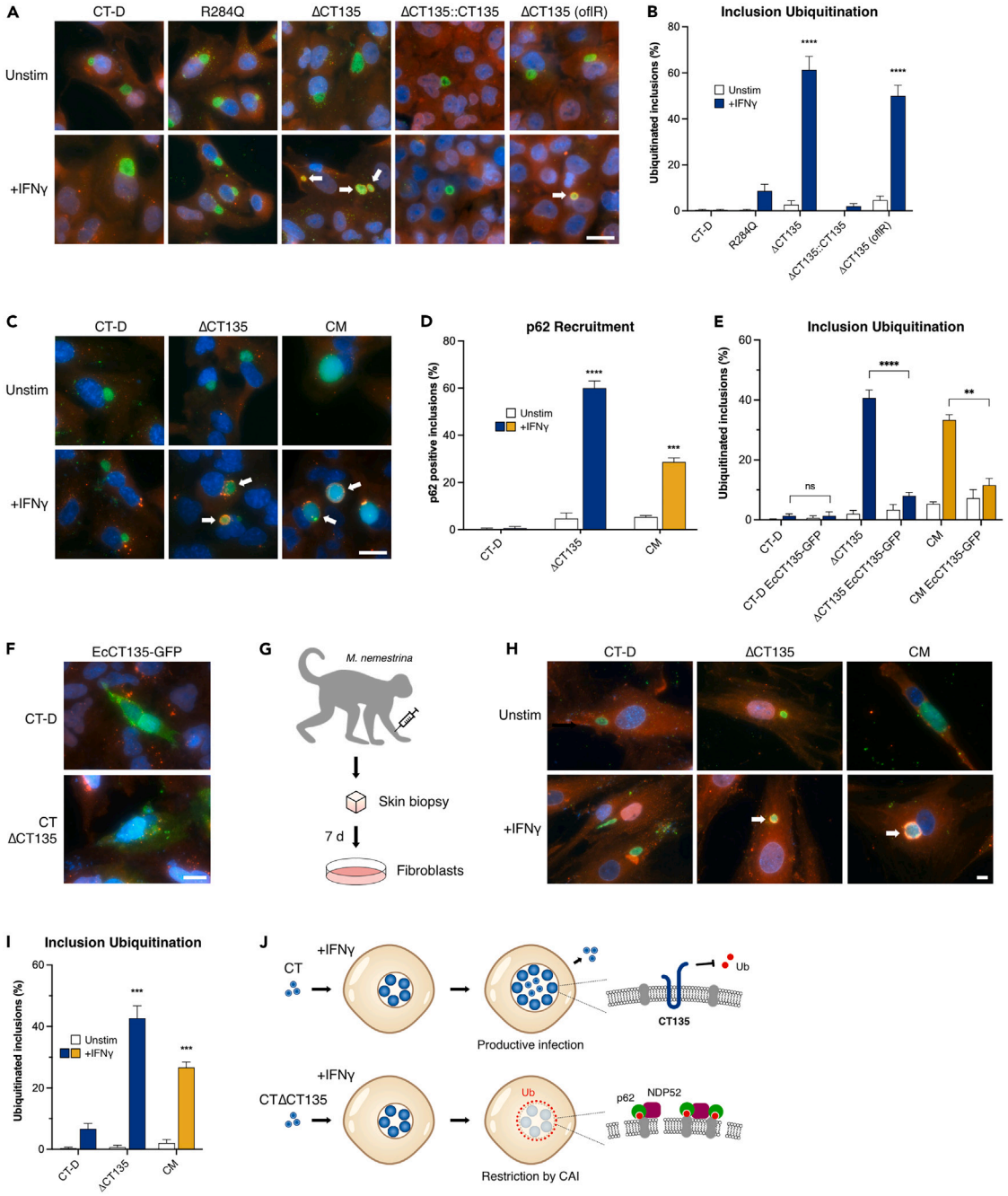

Figure 4. The inclusion membrane protein CT135/GarD is required for CT evasion from cell-autonomous immune defenses

(A) Human cell-autonomous immune defenses target inclusions containing CTΔCT135 at 20 hpi (anti-ubiquitin, red; anti-MOMP, green; DAPI, blue). Restoration of CTΔCT135 with a wild type CT135 allele rescues the defect. Arrows indicate ubiquitinated inclusions. Scale bar, 20 μm.

(B) Quantitative assessment of IFNγ-mediated targeting of ubiquitin to CTΔCT135 inclusions in A549 cells (mean ± SEM, $n = 3$, unpaired Student's t test).

(C) p62/SQSTM (anti-p62, red) is recruited to CTΔCT135 and CM inclusions in a IFNγ-dependent manner (anti-MOMP, green; DAPI, blue). Arrows indicate cells with pronounced p62 recruitment to inclusion membranes. Scale bar, 20 μm.

(D) Quantitative analysis of p62 recruitment in *Chlamydia* infected A549 cells (mean ± SEM, $n = 3$, unpaired Student's t test).

(E) Quantitative evaluation of inclusion ubiquitination in A549 cells ectopically transfected with CT135-GFP and subsequently infected with CT, CTΔCT135, or CM (mean ± SEM, $n = 3$, unpaired Student's t test).

(F) Subcellular distribution of transfected CT135-GFP (green) in A549 cells subsequently infected with CT or CTΔCT135.

(G) Isolation of primary skin fibroblasts from pig-tailed macaques.

Figure 4. *Continued*

(H) IFNγ-induced targeting of CTΔCT135 and CM inclusions in primary macaque cells is conserved with the human pathway (anti-ubiquitin, red; anti-MOMP, green; DAPI, blue). Arrows indicate ubiquitinated inclusions. Scale bar, 20 μm.

(I) Quantitative summary of ubiquitin-mediated targeting of CTΔCT135 and CM inclusions in macaque cells (mean ± SEM, $n = 3$, unpaired Student's t test).

(J) Model of human and NHP CAI evasion by CT135.

in vivo.[14] We analyzed whether p62 was deposited onto CTΔCT135 inclusions in IFNγ-stimulated human cells by immunofluorescence microscopy, and found that under IFNγ-activated conditions 60% of CTΔCT135 and 28.7% of CM inclusions exhibited significant recruitment of p62 to inclusion membranes (Figures 4C and 4D). This recruitment was IFNγ-dependent, as only 5.3% and 4.7% of inclusions were p62-positive in unstimulated cells, respectively (Figures 4C and 4D). No recruitment of p62 was observed for inclusions containing wild type CT-D, regardless of IFNγ-stimulation (Figures 4C and 4D). We additionally investigated the recruitment of the autophagy effector protein NDP52 and it exhibited similar IFNγ-dependent recruitment properties to CTΔCT135 vs. CT-D inclusions (data not shown); however, we were unable to detect NDP52 recruitment to CM inclusions as has previously been shown.[13] Based on multiple lines of evidence demonstrating that CT135 is localized to the inclusion membrane after the protein is secreted into the host cell,[6,15] we explored whether this subcellular localization was necessary for downstream subversion of cell autonomous immune defenses. We transiently transfected A549 cells with a CT135-GFP expression vector to allow for diffuse protein expression throughout the cell that was unrestricted from inclusion membrane localization in infected cells. IFNγ-activated cells with ectopically expressed CT135-GFP and infected with CTΔCT135 exhibited significantly reduced frequencies of ubiquitinated inclusions compared to control cells lacking CT135-GFP ectopic expression (Figure 4E), suggesting that the effector protein does not need to be present on the inclusion membrane in order to partially rescue the ΔCT135 defect. Furthermore, cells that ectopically expressed CT135-GFP yielded reduced IFNγ-mediated targeting of CM inclusions (Figure 4E).

NHPs employ a human-like cell-autonomous immune response

The genes important for human cell-autonomous immunity are conserved in NHPs, but their functional involvement in this model organism has not been explored. This is an important question given that *Chlamydia* resistance to cell-autonomous immunity seems to be shaped by coevolution with their specific hosts.[2,13] To begin to connect *in vitro* mechanistic findings with the outcomes obtained from *in vivo* NHP infections, we examined the functional conservation of CT resistance against cell-autonomous immunity between human and NHP cells. We isolated fibroblasts from a skin biopsy taken from a pig-tailed macaque (Figure 4F) and evaluated CT-D and CTΔCT135 phenotypes in these cells. Wild type CT-D was resistant to inclusion targeting with ubiquitin in IFNγ-stimulated NHP fibroblasts, with 6.7% of CT-D inclusions positive for ubiquitination compared to 42.7% of CTΔCT135 inclusions and 26.7% of CM inclusions (Figures 4G and 4H). Innate immune recognition of mutant or CM inclusions in NHP cells was IFNγ-dependent (Figures 4G and 4H). The IFNγ-dependent mechanism of ubiquitin recruitment to CTΔCT135 and CM inclusions supports our hypothesis that NHP cells can execute a cell-autonomous immune response that is functionally similar to that of humans. These data are the first direct evidence of IFNγ-stimulated NHP cell-autonomous immunity and provides a possible explanation for the *in vivo* attenuation of CTΔCT135 mutants with a failure to evade this pathway.

DISCUSSION

This study demonstrates that the secreted CT inclusion membrane protein CT135 plays a critical role in pathogen-mediated resistance to IFNγ-stimulated cell-autonomous immunity in human cells. We show that CT strains with deleterious mutations in *ct135* were acutely sensitive to recognition and targeting of their resident inclusion membranes with ubiquitin and the autophagy-associated protein p62/SQSTM. Furthermore, disruption of CT135 led to severe developmental growth defects as ΔCT135 mutants had significantly reduced infectious progeny formation in cells exposed to IFNγ. *In vivo* challenge experiments demonstrate that strains defective in CT135 production were unable to successfully establish a productive infection in the female reproductive tracts of NHPs. This underscores the important role of this protein as a CT virulence factor and indicates that humans and NHPs possess conserved IFNγ-activated intracellular strategies for combating CT infection. We also show that the ΔCT135 fitness defect extends to impaired resistance against cell-autonomous immunity in primary nonhuman primate cells. Importantly, our findings agree strongly with recently published findings that reported similar *in vitro* defects for a CT LGV mutant strain deficient for expression of CT135.[15] The combined findings of both studies reinforce the key functional role of CT135 in disrupting host targeting of CT inclusions, and we support the proposed naming of the CT135 protein as GarD (gamma resistance determinant).

Prior work on the relationship between cell-autonomous immunity and *Chlamydia* infection has largely focused on the mouse model. In mouse cells, IFNγ stimulation promotes the recruitment of ubiquitin and downstream effector proteins to CT inclusions;[2] reciprocally, the rodent pathogen CM is resistant.[2] That opposing phenotypes are seen in different host species is likely an outcome of *Chlamydia* adaptation to their preferred hosts and the evolution of specific strategies to overcome the unique immunology of each host. Our findings support this concept by demonstrating that chlamydial strategies for subverting host and NHP innate immunity are conserved yet divergent from the strategy used by CM for evading murine immunity. A focus of future work should be to determine whether the CM homolog of CT135 (TC0412) fulfills a similar function even though the host effectors of cell-autonomous immunity are markedly different in mice.[16] Our findings do not preclude a virulence role for CT135 in mice. In fact, a very recent publication showed that CT135 may function to activate the NLRP3 inflammasome in murine neutrophils, thereby triggering inflammation and neutrophil cytotoxicity.[17] A noted limitation of this study is that a functional role for IFNγ-driven events in impaired infection and growth of ΔCT135 in macaques has not been formally proven. Even though the *in vitro* phenotype of ΔCT135 mutants in NHP cells is IFNγ-dependent, an alternative mechanism may be responsible for reduced *in vivo* growth.

Resistance to IFNγ-induced cell-autonomous immunity is an emerging topic in microbial pathogenesis, and is not unique to *Chlamydia*. The secreted virulence factor IpaH9.8 from *Shigella flexneri* is capable of ubiquitinating guanylate binding protein 1 (GBP1) to promote its proteasomal degradation.[18] GBP1 is a critical component of IFNγ-stimulated cell-autonomous immunity in humans and mice, and IpaH9.8-mediated degradation of GBPs was also observed in the non-native mouse model.[18] *Mycobacterium tuberculosis* was recently shown to also evade GBP-mediated immunity in the mouse model.[19] Previous work has clearly demonstrated that wild type CT is susceptible to IFNγ-stimulated immune defenses in mouse cells.[2] Therefore, the primate-restricted nature of GarD-mediated resistance suggests that this effector protein interferes with a stage of cell-autonomous immunity that is not shared between primates and mice, in contrast to the partially conserved family of GBPs which are targeted by other pathogens.

A prior study suggested that CT135 was unimportant to CT virulence in NHPs.[20] The data supporting that conclusion were generated by comparing infection outcomes of NHPs inoculated with either D/EC or D/LC strains of CT—at the time, D/LC was thought to encode a functional copy of CT135.[7] Although no significant differences were observed between mutant infections, it was noted that half of monkeys in D/EC and D/LC infected cohorts failed to become infected for unknown reasons and was unexpected for wild type-like CT-D.[20] Our findings show that D/EC and D/LC are equally susceptible to IFNγ-stimulated immunity, to a similar extent as a ΔCT135 strain, and thus are both CT135 mutants. The finding that a ΔCT135 mutant failed to establish an infection in macaques supports this conclusion.

CT135/GarD represents the second CT virulence factor important for resisting the antibacterial effects of IFNγ in human cells, preceded by the tryptophan synthase operon encoded by urogenital CT serovars.[8] This underscores the strong evolutionary pressure put on CT by IFNγ-mediated immunity. Moreover, these distinct virulence mechanisms appear to be specifically tuned to the native human host, as CT fails to overcome IFNγ-stimulated cell-autonomous immunity in the mice, which lack an IFNγ-inducible IDO.[2,21] Sequences from clinical isolates revealed that *ct135* appears to be genetically stable in circulating strains, in contrast to its propensity for acquiring deleterious mutations *in vitro*.[10] While the selective pressure for gene deletion during culture adaptation may be due to slight *in vitro* fitness advantages of *ct135* mutants,[22] the apparent maintenance of this gene in clinical strains supports the importance of this effector for CT virulence and pathogenesis.

Limitations of the study

We highlight three limitations of the study. First, the nonhuman primate study design does not allow direct determination of whether the impaired growth of the *ct135* mutant was due to an IFNγ dependent process. To accomplish this would require a non-genetic experimental strategy for depleting IFNγ from the monkeys, and this was outside the scope of the study. Second, although the described intracellular immune pathways are conserved between NHPs and humans, our use of NHP skin fibroblasts leaves unanswered whether the pathway is similarly active in endocervical epithelial cells. A final noted limitation is that a complete mechanistic understanding for how GarD/CT135 manipulates specific host targets in order to prevent ubiquitination of proteins on or near the inclusion membrane, remains elusive. We also do not have a full appreciation for what proteins on the inclusion membrane are ubiquitinated in IFNγ-activated cells, and whether they represent targets that are reproducibly modified. These outstanding questions should be the focus of long-term follow up investigations.

STAR★METHODS

Detailed methods are provided in the online version of this paper and include the following:

- KEY RESOURCES TABLE
- RESOURCE AVAILABILITY
  - Lead contact
  - Materials availability
  - Data and code availability
- EXPERIMENTAL MODEL AND STUDY PARTICIPANT DETAILS
  - Bacteria strains
  - Cell lines
  - Animals
- METHOD DETAILS
  - *In vitro Chlamydia* infections
  - Immunofluorescence microscopy
  - Progeny production assay
  - Whole genome sequencing
  - Macaca nemestrina infection
  - Derivation of ofl^R CTΔCT135
  - Recombination-mediated rescue of the CTΔCT135 open reading frame
  - Nonhuman primate fibroblast isolation
  - Protein structure prediction
- QUANTIFICATION AND STATISTICAL ANALYSIS

SUPPLEMENTAL INFORMATION

Supplemental information can be found online at https://doi.org/10.1016/j.isci.2024.110143.

ACKNOWLEDGMENTS

We thank M. Gale (University of Washington), Chris English (Washington National Primate Research Center), and H. Caldwell (NIH) for sharing cell lines, tissues, and strains. We thank J. Coers (Duke University) for technical consultation. We thank the Oregon State University Center for Quantitative Life Sciences Sequencing Core for technical support. This work was supported by the National Institutes of Health (NIH) (R01AI126785, R21AI149072, P51OD010425, and T32AI007140).

AUTHOR CONTRIBUTIONS

Conceptualization, M.C.F., Y.C.S., D.L.P., and K.H.; investigation, M.C.F., Y.C.S., R.J.S., S.J.C., and I.Q.P.; writing, M.C.F. and K.H.; visualization, M.C.F., I.Q.P., and K.H.; resources, D.D.R., D.L.P., and K.H.; supervision, D.D.R, D.L.P., and K.H.

DECLARATION OF INTERESTS

The authors declare no competing interests.

Received: January 31, 2024
Revised: April 19, 2024
Accepted: May 27, 2024
Published: May 28, 2024

REFERENCES

1. Finethy, R., and Coers, J. (2016). Sensing the Enemy, Containing the Threat: Cell-Autonomous Immunity to Chlamydia trachomatis (Oxford University Press). https://doi.org/10.1093/femsre/fuw027.
2. Haldar, A.K., Foltz, C., Finethy, R., Piro, A.S., Feeley, E.M., Pilla-Moffett, D.M., Komatsu, M., Frickel, E.M., and Coers, J. (2015). Ubiquitin systems mark pathogen-containing vacuoles as targets for host defense by guanylate binding proteins. Proc. Natl. Acad. Sci. USA *112*, E5628–E5637. https://doi.org/10.1073/pnas.1515966112.
3. Haldar, A.K., Piro, A.S., Finethy, R., Espenschied, S.T., Brown, H.E., Giebel, A.M., Frickel, E.M., Nelson, D.E., and Coers, J. (2016). Chlamydia trachomatis Is Resistant to Inclusion Ubiquitination and Associated Host Defense in Gamma Interferon-Primed Human Epithelial Cells. mBio *7*, e01417-16. https://doi.org/10.1128/mbio.01417-16.
4. Bakshi, R.K., Gupta, K., Jordan, S.J., Chi, X., Lensing, S.Y., Press, C.G., and Geisler, W.M. (2018). An Adaptive Chlamydia trachomatis-Specific IFN-γ-Producing CD4 + T Cell Response Is Associated With Protection Against Chlamydia Reinfection in Women. Front. Immunol. *9*, 1981. https://doi.org/10.3389/fimmu.2018.01981.
5. Suchland, R.J., Carrell, S.J., Wang, Y., Hybiske, K., Kim, D.B., Dimond, Z.E., Hefty, P.S., and Rockey, D.D. (2019). Chromosomal recombination targets in Chlamydia interspecies lateral gene transfer. J. Bacteriol. *201*, 1–15. https://doi.org/10.1128/JB.
6. Weber, M.M., Bauler, L.D., Lam, J., and Hackstadt, T. (2015). Expression and localization of predicted inclusion membrane proteins in Chlamydia trachomatis. Infect. Immun. *83*, 4710–4718. https://doi.org/10.1128/IAI.01075-15.
7. Sturdevant, G.L., Kari, L., Gardner, D.J., Olivares-Zavaleta, N., Randall, L.B., Whitmire, W.M., Carlson, J.H., Goheen, M.M., Selleck, E.M., Martens, C., and Caldwell, H.D. (2010). Frameshift mutations in a single novel virulence factor alter the *in vivo* pathogenicity of Chlamydia trachomatis for the female murine genital tract. Infect. Immun. *78*, 3660–3668. https://doi.org/10.1128/IAI.00386-10.
8. Nelson, D.E., Virok, D.P., Wood, H., Roshick, C., Johnson, R.M., Whitmire, W.M., Crane, D.D., Steele-Mortimer, O., Kari, L., McClarty, G., and Caldwell, H.D. (2005). Chlamydial IFN-γ immune evasion is linked to host infection tropism. Proc. Natl. Acad. Sci. USA *102*, 10658–10663. https://doi.org/10.1073/PNAS.0504198102.
9. Wolner-Hanssen, P., Patton, D.L., and Holmes, K.K. (1991). Protective immunity in pig-tailed macaques after cervical infection with Chlamydia trachomatis. Sex. Transm. Dis. *18*, 21–25. https://doi.org/10.1097/00007435-199101000-00005.
10. Bonner, C., Caldwell, H.D., Carlson, J.H., Graham, M.R., Kari, L., Sturdevant, G.L., Tyler, S., Zetner, A., and Mcclarty, G. (2015). Chlamydia trachomatis virulence factor CT135 is stable *in vivo* but highly polymorphic *in vitro*. Pathog. Dis. *73*, ftv043. https://doi.org/10.1093/femspd/ftv043.
11. Jumper, J., Evans, R., Pritzel, A., Green, T., Figurnov, M., Ronneberger, O., Tunyasuvunakool, K., Bates, R., Žídek, A., Potapenko, A., et al. (2021). Highly accurate protein structure prediction with AlphaFold. Nature *596*, 583–589. https://doi.org/10.1038/S41586-021-03819-2.
12. Mirdita, M., Schütze, K., Moriwaki, Y., Heo, L., Ovchinnikov, S., and Steinegger, M. (2021). ColabFold - Making protein folding accessible to all. Preprint at bioRxiv. https://doi.org/10.1101/2021.08.15.456425.
13. Haldar, A.K., Piro, A.S., Finethy, R., Espenschied, S.T., Brown, H.E., Giebel, A.M., Frickel, E.M., Nelson, D.E., and Coers, J. (2016). Chlamydia trachomatis is resistant to inclusion ubiquitination and associated host defense in gamma interferon-primed human epithelial cells. mBio *7*, e01417-16. https://doi.org/10.1128/mBio.01417-16.
14. Lee, Y., Sasai, M., Ma, J.S., Sakaguchi, N., Ohshima, J., Bando, H., Saitoh, T., Akira, S., and Yamamoto, M. (2015). p62 Plays a Specific Role in Interferon-γ-Induced Presentation of a Toxoplasma Vacuolar Antigen. Cell Rep. *13*, 223–233. https://doi.org/10.1016/J.CELREP.2015.09.005.
15. Walsh, S.C., Reitano, J.R., Dickinson, M.S., Kutsch, M., Hernandez, D., Barnes, A.B., Schott, B.H., Wang, L., Ko, D.C., Kim, S.Y., et al. (2022). The bacterial effector GarD shields Chlamydia trachomatis inclusions from RNF213-mediated ubiquitylation and destruction. Cell Host Microbe *30*, 1671–1684.e9. https://doi.org/10.1016/j.chom.2022.08.008.
16. Bekpen, C., Marques-Bonet, T., Alkan, C., Antonacci, F., Leogrande, M.B., Ventura, M., Kidd, J.M., Siswara, P., Howard, J.C., and Eichler, E.E. (2009). Death and Resurrection of the Human IRGM Gene. PLoS Genet. *5*, e1000403. https://doi.org/10.1371/JOURNAL.PGEN.1000403.
17. Yang, C., Lei, L., Collins, J.W.M., Briones, M., Ma, L., Sturdevant, G.L., Su, H., Kashyap, A.K., Dorward, D., Bock, K.W., et al. (2021). Chlamydia evasion of neutrophil host defense results in NLRP3 dependent myeloid-mediated sterile inflammation through the purinergic P2X7 receptor. Nat. Commun. *12*, 5454. https://doi.org/10.1038/S41467-021-25749-3.
18. Li, P., Jiang, W., Yu, Q., Liu, W., Zhou, P., Li, J., Xu, J., Xu, B., Wang, F., and Shao, F. (2017). Ubiquitination and degradation of GBPs by a Shigella effector to suppress host defence. Nature *551*, 378–383. https://doi.org/10.1038/nature24467.
19. Olive, A.J., Smith, C.M., Baer, C.E., Coers, J., and Sassetti, C.M. (2020). Mycobacterium tuberculosis evasion of Guanylate Binding Protein-mediated host defense in mice requires the ESX1 secretion system. Preprint

at bioRxiv. https://doi.org/10.1101/2020.07.27.223362.

20. Patton, D.L., Sweeney, Y.C., Baldessari, A.E., Cles, L., Kari, L., Sturdevant, G.L., Yang, C., and Caldwell, H.D. (2018). The Chlamydia trachomatis plasmid and CT135 virulence factors are not essential for genital tract infection or pathology in female pig-tailed macaques. Infect. Immun. *86*, e00121-18. https://doi.org/10.1128/IAI.00121-18.
21. Roshick, C., Wood, H., Caldwell, H.D., and McClarty, G. (2006). Comparison of Gamma Interferon-Mediated Antichlamydial Defense Mechanisms in Human and Mouse Cells. Infect. Immun. *74*, 225–238. https://doi.org/10.1128/IAI.74.1.225-238.2006.
22. Borges, V., Pinheiro, M., Antelo, M., Sampaio, D.A., Vieira, L., Ferreira, R., Nunes, A., Almeida, F., Mota, L.J., Borrego, M.J., and Gomes, J.P. (2015). Chlamydia trachomatis In Vivo to In Vitro Transition Reveals Mechanisms of Phase Variation and Down-Regulation of Virulence Factors. PLoS One *10*, e0133420. https://doi.org/10.1371/JOURNAL.PONE.0133420.
23. Wang, Y., LaBrie, S.D., Carrell, S.J., Suchland, R.J., Dimond, Z.E., Kwong, F., Rockey, D.D., Hefty, P.S., and Hybiske, K. (2019). Development of Transposon Mutagenesis for Chlamydia muridarum. J. Bacteriol. *201*, e00366-19. https://doi.org/10.1128/JB.00366-19.
24. Bolger, A.M., Lohse, M., and Usadel, B. (2014). Trimmomatic: a flexible trimmer for Illumina sequence data. Bioinformatics *30*, 2114–2120. https://doi.org/10.1093/BIOINFORMATICS/BTU170.
25. Zerbino, D.R., and Birney, E. (2008). Velvet: algorithms for *de novo* short read assembly using de Bruijn graphs. Genome Res. *18*, 821–829. https://doi.org/10.1101/gr.074492.107.
26. Langmead, B., and Salzberg, S.L. (2012). Fast gapped-read alignment with Bowtie 2. Nat. Methods *9*, 357–359. https://doi.org/10.1038/nmeth.1923.
27. Baek, M., DiMaio, F., Anishchenko, I., Dauparas, J., Ovchinnikov, S., Lee, G.R., Wang, J., Cong, Q., Kinch, L.N., Schaeffer, R.D., et al. (2021). Accurate prediction of protein structures and interactions using a three-track neural network. Science *373*, 871–876. https://doi.org/10.1126/SCIENCE.ABJ8754.
28. Kim, D.E., Chivian, D., and Baker, D. (2004). Protein structure prediction and analysis using the Robetta server. Nucleic Acids Res. *32*, W526–W531. https://doi.org/10.1093/NAR/GKH468.
29. Pettersen, E.F., Goddard, T.D., Huang, C.C., Meng, E.C., Couch, G.S., Croll, T.I., Morris, J.H., and Ferrin, T.E. (2021). UCSF ChimeraX: Structure visualization for researchers, educators, and developers. Protein Sci. *30*, 70–82. https://doi.org/10.1002/PRO.3943.

STAR★METHODS

KEY RESOURCES TABLE

REAGENT or RESOURCE	SOURCE	IDENTIFIER
Antibodies		
Mouse anti C. trachomatis MOMP	Virostat	Cat# 1621
anti-Ubiquitin	Enzo Life Sciences	Cat# BML-PW8810-0500; RRID: AB_2051891
anti-p62	Abcam	Cat# ab109012; RRID: AB_2810880
anti-NDP52	Abcam	Cat# ab68588; RRID: AB_1640255
Goat anti-Mouse IgG (H + L) Cross-Adsorbed Secondary Antibody, Alexa Fluor™ 488	Invitrogen	Cat# A11001; RRID: AB_2534069
Donkey anti-Goat Alexa Fluor 488	Invitrogen	Cat# A11055; RRID: AB_2534102
Donkey anti-Rabbit Alexa Fluor 594	Invitrogen	Cat# A21207; RRID: AB_141637
Rabbit anti-Mouse Alexa Fluor 594	Invitrogen	Cat# A11062; RRID: AB_2534109
Bacterial and virus strains		
Chlamydia trachomatis LGV L2/434/Bu	University of Washington	N/A
Chlamydia trachomatis D/UW-3/CX	University of Washington	N/A
Chlamydia trachomatis D/6319	University of Washington	N/A
Chlamydia trachomatis J/p225	University of Washington	N/A
Chlamydia trachomatis D/EC	Harlan Caldwell	N/A
Chamydia trachomatis D/LC	Harlan Caldwell	N/A
Chlamydia trachomatis D/6319 ΔCT135	Isolated this study	N/A
Chlamydia trachomatis D/6319 R284Q	Isolated this study	N/A
Chlamydia trachomatis D/6319 nt1034	Isolated this study	N/A
Chlamydia muridarum Nigg	University of Washington	N/A
Chlamydia trachomatis L2:Tn386	University of Washington	N/A
Chlamydia muridarum GFP	University of Washington	N/A
Biological samples		
Macaque (Macaca nemestrina)	WaNPRC	N/A
Chemicals, peptides, and recombinant proteins		
Human interferon gamma	R&D Systems	Cat# 285-IF-100
Tryptophan	Sigma	Cat# T0254
Dulbecco's high glucose modified Eagles medium	Thermo Fisher	Cat# SH30022LS
RQ1 DNase	Promega	Cat# M6101
DNeasy blood & tissue kit	Qiagen	Cat# 69504
Nextera XT DNA library preparation kit	Illumina	Cat# FC-131-1096
Critical commercial assays		
Aptima Combo 2 assay	Hologic	Cat# PRD-05576
Deposited data		
BQ06_D0_J_p225 pre-inoc	NCBI	GenBank: CP156063
BQ06_K06160_J_p225 5 wpi isolate	NCBI	GenBank: CP156064
BQ06_L04117_J_p225 5 wpi isolate	NCBI	GenBank: CP156065
BQ07_D0_D_6319 pre-inoc	NCBI	GenBank: CP156067
BQ07_A11257_D_6319 5 wpi isolate	NCBI	GenBank: CP156066

(*Continued on next page*)

Continued

REAGENT or RESOURCE	SOURCE	IDENTIFIER
Experimental models: Cell lines		
A549 cells	Michael Gale, University of Washington	ATCC CCL-185
McCoy cells	University of Washington	ATCC CRL-1696
Primary NHP fibroblasts	WaNPRC	N/A
Recombinant DNA		
CT135	*C. trachomatis* D/UW3, University of Washington	N/A
Software and algorithms		
Prism 10	GraphPad	N/A
RoseTTAFold	Robetta server	N/A
AlphaFold2-advanced	University of Washington	N/A
ChimeraX	UCSF	N/A
Trimmomatic	USADELLAB.org	N/A
Velvet	Github	N/A
Bowtie2	Johns Hopkins University	N/A
Geneious	Dotmatics	N/A

RESOURCE AVAILABILITY

Lead contact

Further information and requests for resources and reagents should be directed to and will be fulfilled by the lead contact, Kevin Hybiske (khybiske@uw.edu).

Materials availability

CT strains and expression plasmids generated in this study are available upon request.

Data and code availability

- CT genome sequence data have been deposited at NCBI and are publicly available as of the date of publication. Accession numbers are listed in the key resources table.
- This paper does not report original code.
- Any additional information required to reanalyze the data reported in this paper is available from the lead contact upon request

EXPERIMENTAL MODEL AND STUDY PARTICIPANT DETAILS

Bacteria strains

CT strains used in this study include CT LGV L2 434/Bu, D UW-3/CX, D/6319, J/p225, CT-D/EC, and CT-D/LC. The CM strain used in this study encodes green fluorescent protein (GFP) on a transposon inserted in an intergenic region of its genome.[23] Generation of our chimera library is described in detail in a previous publication.[5]

Cell lines

A549 cells (ATCC CCL-185) were obtained from Michael Gale and McCoy cells (ATCC CRL-1696) were obtained from Walt Stamm. Primary NHP fibroblasts were cultured in standard conditions.

Animals

Nine sexually mature female pig-tailed macaques (*Macaca nemestrina*) age 5–11 years were used in the study. All monkeys were housed at the Washington National Primate Research Center. Prior approval for use of monkeys in this protocol was obtained from the Institutional Animal Care and Use Committee at the University of Washington. The animals were monitored daily for one month after assignment, for general health and to document normal menstrual cycles. The use and care of animals for this study followed the guidelines by the University of Washington Institutional Animal Care and Use Committee.

METHOD DETAILS

In vitro Chlamydia infections

Infection of host cells in this study was performed by diluting *Chlamydia* EBs in tissue culture medium and adding to adherent host cells in tissue culture plates or chamber slides, which were then centrifuged at 700 × *g*. Infections were performed in DMEM media under 37°C with 5% CO_2 condtions, for times indicated in each experiment.

Immunofluorescence microscopy

Chambered coverglass slides (8-well Nunc Lab-Tek II; Thermo Fisher Scientific, Rockford, IL) were seeded with A549 cells or primary NHP fibroblasts and cultured at 37°C, 5% CO_2. Cells were infected with *Chlamydia* strains such that three technical replicates are represented in final data. Wells were left either untreated or stimulated with 100U/mL human interferon gamma (IFNγ, R&D Systems, Minneapolis, MN; 285-IF-100) at 3 h post infection (hpi). Infected cells were fixed at 20 hpi with 3.7% paraformaldehyde for 20 min, washed 3 times with phosphate buffered saline (PBS), and permeabilized with 0.5% Triton X-100 for 15 min. Wells were washed once more and blocked with 3% bovine serum albumin (BSA) in PBS for 1 h. Primary antibodies were diluted (dilution factors listed under 'Antibodies and Reagents') in 1% BSA-PBS and incubated at room temperature for 1 h, after which we performed 3 5-min washes before adding secondary antibodies. Secondary antibodies and DAPI were diluted (dilution factors listed under 'Antibodies and Reagents') in 1% BSA-PBS and incubated for 45 min at room temperature in the dark. We performed 3 5-min washes with PBS and slides were imaged in PBS and stored at 4°C. Stained chamber slides were imaged on a Nikon Ti-E inverted microscope. Images were captured with a Hamamatsu camera controller C10600, and visualized using Volocity software (PerkinElmer, Waltham, MA). For inclusion-recruitment assays, 50 inclusions were counted in each well, and each inclusion was positive for ubiquitin or p62 recruitment if there was a complete ring clearly visible around the inclusion. Inclusions were called positive for NDP52 if there were complete or partial rings around around them, which is consistent with published findings.[13] The data in our recruitment assay represent the number of ubiquitin, p62, or NDP52-positive inclusions divided by 50 (the total number of inclusions counted in each well). Data are representative of 3 technical replicates. Immunofluorescence images in figures are representative of the annotated strains/conditions. The microscopist was not blinded to conditions.

Progeny production assay

Human A549 cells were pretreated overnight with either DMEM supplemented with IFNγ (100 U/mL) plus tryptophan (Trp, 100 μg/mL) or with Trp only. Pretreated cells were infected with CT-D, CM-GFP, CT-D/EC, or CT-D/LC. At 27 hpi, EBs were extracted from infected cells and serially diluted into 96 well plates seeded with confluent monolayers of McCoy murine fibroblasts. These plates were centrifuged at 700 × *g* and incubated in DMEM at 37°C, 5% CO_2. At 24 hpi, infected cells were fixed, permeabilized, and stained with an anti-MOMP antibody (Virostat) followed by a secondary antibody conjugated to Alexa Fluor 488 (Thermo Fisher Scientific) for visualization of CT inclusions. CM inclusions were visualized through their expression of GFP. Inclusion counts per field was quantitatively measured via immunofluorescence microscopy to calculate inclusion forming units per mL of the original lysates. Dilutions containing 10–100 inclusions per field were selected, and three fields were counted per strain/condition. IFU/mL in IFNγ + Trp pretreated conditions were divided by the IFU/mL in Trp-only conditions for each *Chlamydia* strain tested and the resulting ratio was reported as % progeny production in IFNγ-stimulated cells.

Whole genome sequencing

Chlamydia EBs were centrifuged at 16,000 × *g* for 10 min and supernatants were discarded. The resulting pellet was resuspended in water and treated with RQ1 DNase (Promega) at 37°C for 30 min, and then RQ1 stop solution was added for 10 min at 65°C. Dithiothreitol was added for a final concentration of 5 mM, and the lysates were incubated at 56°C for 1 h in a shaker. Genomic DNA was then extracted using a DNeasy blood and tissue kit (Qiagen), as per the manufacturers instructions. Whole-genome-sequencing templates were prepared using a Nextera XT DNA library preparation (Illumina). Genome sequencing was conducted on an Illumina HiSeq 3000 at the Oregon State University Center for Genome Research and Biocomputing Core. The Illumina-generated reads were filtered and trimmed to remove low quality reads using Trimmomatic.[24] The manicured read files were assembled into contigs with Velvet V 1.2.10[25] and assembled using the bioinformatics software platform Geneious. The resulting genomes were confirmed by remapping the reads with Bowtie2[26] to the assembled genomes. Given the high genomic similarities between CT-L2 and CT-D, recombination ends were approximated by determining the presence of differentiating SNPs of sequenced strains.

Macaca nemestrina infection

Six pig-tailed macaques were infected with a single CT-D inoculum (D/6319) in this study, six animals were infected with a single CT-J inoculum (J/p225), one animal was infected with a single CTΔCT135 inoculum, and two animals were infected with five sequential inocula of CTΔCT135. Animals were inoculated with 1 mL (10^5 IFU) of CT by expelling a 1 cc tuberculin syringe into the vaginal fornix. Animals were monitored weekly for active chlamydia infection by culture and nucleic acid amplification tests (NAATs). Animals were considered actively infected if they were culture and/or NAAT positive during weekly testing. At the end of the study, infected animals were treated with azithromycin (14 mg/kg for 5 days) regardless of positivity by culture or NAAT.

Derivation of ofl^R CTΔCT135

To derive an oflaxacin-resistant (ofl^R) strain of the CTΔCT135 mutant, we inoculated McCoy cells with CTΔCT135 (serovar D background) EBs in 75 cm^2 flasks and initiated infection by centrifuging the flasks at 1,200 x *g* for 1 h at 37°C. Infected cells were fed with subinhibitory levels of ofloxacin equivalent to half of its MIC (0.25 μg/mL) and incubated at 37°C and 5% CO_2 for 48 h. Cell layers were disrupted by freeze-thawing at −80°C and 37°C followed by gentle aspiration with a micropipette and low-speed centrifugation to remove debris. Supernatants from these disrupted cells were passaged onto fresh McCoy cell monolayers in 12-mm^2 shell vials to select for resulting mutants. Serial 2-fold dilutions of ofloxacin diluted in minimal essential medium supplemented with 10% fetal bovine serum and cycloheximide (1ug/mL) (MEM-10) were added to infected cells in shell vials. Resistance was monitored using immunofluorescence microscopy following culture in 48-well tissue culture plates. When resistant inclusions appeared, CTΔCT135-ofl^R was clonally isolated by limiting dilution.

Recombination-mediated rescue of the CTΔCT135 open reading frame

Recombination experiments were performed in shell vials (12mm^2) seeded with 4.0 x 10^5 McCoy cells. These monolayers were coinfected with CTΔCT135-ofl^R and a previously generated tetracycline-resistant (tet^R) transposon mutant in a *C. trachomatis* serovar L2 background (CtL2Tn). CtL2Tn encodes a tet^R transposon in *ctl0386* (homologue of serovar D *ct131*). Monolayers of McCoy cells were infected with approximate multiplicity of infection of 2.0 of each CTΔCT135 and CtL2Tn. Cultures were incubated for 48 h at 37°C and 5% CO_2 in the absence of antibiotics, then they were harvested by the freeze-thaw method described above. Recombinant strains were isolated by inoculating 50uL of lysates from shell vials into McCoy monolayers in new shell vials and were incubated at 37°C and 5% CO_2 in MEM-10 supplemented with 2ug/mL ofloxacin and 0.5ug/mL tetracycline—representing 4x and 2x the MIC of parental strains, respectively. Cultures were grown for 48 h and surviving bacteria were detected by immunofluorescence. Infected cells were lysed by the freeze-thaw method and blindly passaged until inclusions were observed by immunofluorescence microscopy. Recovered dual-resistant strains were cloned by limiting 2-fold dilution and recombinants with a predominantly CTΔCT135 genome were determined by serological typing of MOMP by immunofluorescence microscopy. A total of ten tet^R/ofl^R recombinants were isolated, and we screened for *ct135* rescue by Sanger sequencing followed by a phenotype screen performing our ubiquitination assay detailed above.

Nonhuman primate fibroblast isolation

A skin biopsy from a 5-year-old female pigtailed macaque was acquired from the Washington National Primate Research Center's Tissue Distribution Program. The skin was immediately submerged in 30mL of DMEM supplemented with GlutaMax and 20% FBS (DMEMp) and transported on ice for processing. The skin was dissected into ~2mm^3 sections, and 2–3 pieces were added to each well of 6-well plates that had been coated with a 1% gelatin solution for 30 min at room temperature. The sections were partially submerged in 800uL of DMEMp supplemented with 1x PenStrep (Thermo Fisher Scientific) and incubated at 37°C, 5% CO_2 for one week to allow attachment of skin and outgrowth of fibroblasts. After one week, the volume of DMEMp + 1x PenStrep was increased to 2mL/well. Once confluent, cells were trypsinized and each 6-well plate was split into two 75cm^2 tissue culture flasks. These cells were washed thoroughly with PBS and passaged into additional 75cm^2 flasks and grown in DMEMc (without PenStrep). One additional passage was performed in the absence of PenStrep, and once cells were ~70–80% confluent, flasks were washed with PBS, trypsinized, and cells were either cryopreserved in DMEMc +10% DMSO, passaged into 75cm^2 flasks or used to seed 8-well chamber slides for ubiquitination assays as described above. Infection with *Chlamydia* strains was performed as described above for human cells.

Protein structure prediction

RoseTTAFold[27] models were generated through the Robetta server[28] using default parameters. AlphaFold2-advanced[11,12] models were obtained with num_samples = 4 and is_training = True to increase sampling, and optimized max_recycles = 12. Models were visualized and analyzed with ChimeraX.[29]

QUANTIFICATION AND STATISTICAL ANALYSIS

GraphPad Prism software was used for all statistical analyses, with both unpaired t and Wilcoxon tests used for group comparisons. In all instances the data reported are mean measurements and error bars denote the SEM values (*$p < 0.05$, **$p < 0.005$, ***$p < 0.001$, ****$p < 0.0001$).